

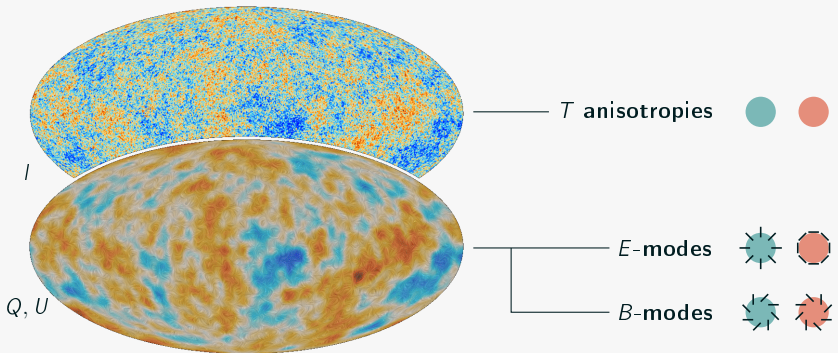
Impact of half-wave plate systematics on the measurement of cosmic birefringence from CMB polarization

Marta Monelli

Max Planck Institut für Astrophysik
Garching (Germany)

February 3rd, 2023

CMB anisotropies

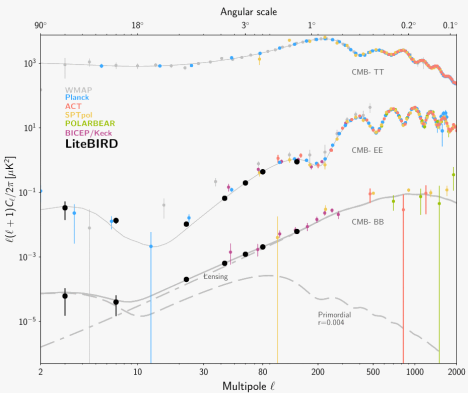


searching B -modes from inflation

Expectation: inflation-sourced perturbations leave traces on the CMB polarization.

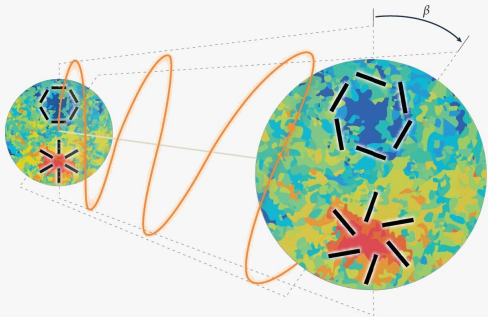
Large scale B -modes can probe inflation.

Unprecedented sensitivity requirements!



a side effect: measuring cosmic birefringence

CMB might also carry information about parity-violating new physics: **cosmic birefringence**.
(time-dependent parity-violating pseudoscalar field)



mixing of E and B modes:

$$\begin{cases} a_{\ell m, \text{obs}}^E = a_{\ell m}^E \cos 2\beta - a_{\ell m}^B \sin 2\beta, \\ a_{\ell m, \text{obs}}^B = a_{\ell m}^E \sin 2\beta + a_{\ell m}^B \cos 2\beta. \end{cases}$$

trying to constrain β

$$\left\{ \begin{array}{l} C_{\ell,\text{obs}}^{TT} = C_\ell^{TT}, \\ C_{\ell,\text{obs}}^{EE} = \cos^2(2\beta)C_\ell^{EE} + \sin^2(2\beta)C_\ell^{BB} - \sin(4\beta)C_\ell^{EB}, \\ C_{\ell,\text{obs}}^{BB} = \cos^2(2\beta)C_\ell^{BB} + \sin^2(2\beta)C_\ell^{EE} + \sin(4\beta)C_\ell^{EB}, \\ C_{\ell,\text{obs}}^{TE} = \cos(2\beta)C_\ell^{TE} - \sin(2\beta)C_\ell^{TB}, \\ C_{\ell,\text{obs}}^{EB} = \sin(4\beta)(C_\ell^{EE} - C_\ell^{BB})/2 + \cos(4\beta)C_\ell^{EB}, \\ C_{\ell,\text{obs}}^{TB} = \sin(2\beta)C_\ell^{TE} + \cos(2\beta)C_\ell^{TB}. \end{array} \right.$$

$C_{\ell,\text{obs}}^{EB} = \tan(4\beta)(C_{\ell,\text{obs}}^{EE} - C_{\ell,\text{obs}}^{BB})/2.$



trying to constrain β

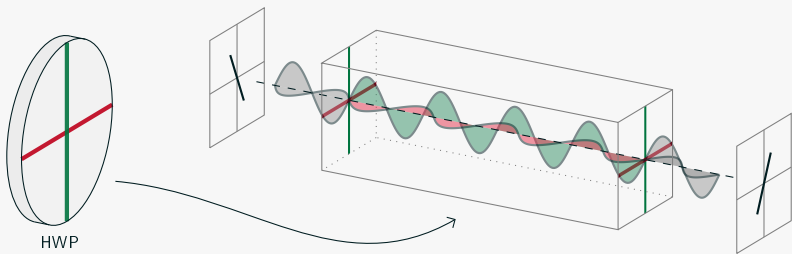
$$\begin{cases} C_{\ell,\text{obs}}^{TT} = C_\ell^{TT}, \\ C_{\ell,\text{obs}}^{EE} = \cos^2(2\beta)C_\ell^{EE} + \sin^2(2\beta)C_\ell^{BB} - \sin(4\beta)C_\ell^{EB}, \\ C_{\ell,\text{obs}}^{BB} = \cos^2(2\beta)C_\ell^{BB} + \sin^2(2\beta)C_\ell^{EE} + \sin(4\beta)C_\ell^{EB}, \\ C_{\ell,\text{obs}}^{TE} = \cos(2\beta)C_\ell^{TE} - \sin(2\beta)C_\ell^{TB}, \\ C_{\ell,\text{obs}}^{EB} = \sin(4\beta)(C_\ell^{EE} - C_\ell^{BB})/2 + \cos(4\beta)C_\ell^{EB}, \\ C_{\ell,\text{obs}}^{TB} = \sin(2\beta)C_\ell^{TE} + \cos(2\beta)C_\ell^{TB}. \end{cases}$$

→ $C_{\ell,\text{obs}}^{EB} = \tan(4\beta)(C_{\ell,\text{obs}}^{EE} - C_{\ell,\text{obs}}^{BB})/2.$

$$\beta = 0.35 \pm 0.14 \text{ (68%CL)}$$

**To extract this kind of information from CMB
systematics have to be kept under control.**

the HWP: reducing systematics



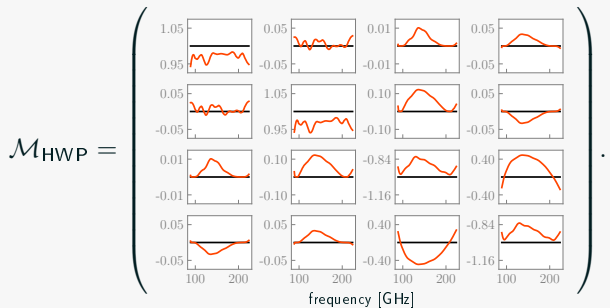
A **rotating** half-wave plate (HWP) as first optical element:

- ▶ modulates the signal to $4f_{\text{HWP}}$, allowing to “escape” $1/f$ noise;
- ▶ makes possible for a single detector to measure polarization, reducing pair-differencing systematics.

the HWP: inducing systematics

Mueller calculus: radiation described as $S = (I, Q, U, V)$, effect of polarization-altering devices parametrized by \mathcal{M} : so that $S' = \mathcal{M} \cdot S$.

For an ideal HWP, $\mathcal{M}_{\text{ideal}} = \text{diag}(1, 1, -1, -1)$, but let's look at a realistic case:



how does this affect the observed maps?

steps we took in that direction

- ▶ work on a simulation pipeline for a LiteBIRD-like mission;
- ▶ simulate observed maps in presence of non-ideal HWP;
- ▶ derive analytical formulae to interpret the output.

PREPARED FOR SUBMISSION TO JCAP

Impact of half-wave plate systematics on the measurement of cosmic birefringence from CMB polarization

Marta Monelli,^a Eiichiro Komatsu,^{a,b} Alexandre Adler,^c Matteo
Billi,^{d,e,f} Paolo Campeti,^{a,g} Nadia Dachlythra,^c Adriaan
Duivenvoorden,^h Jon Gudmundsson,^c and Martin Reinecke.^a

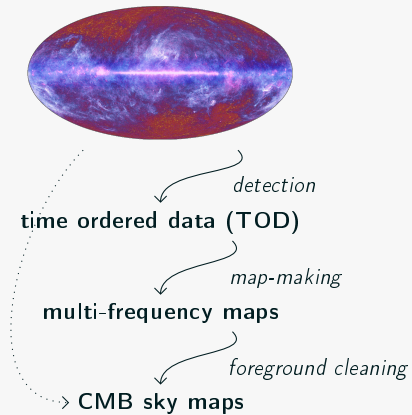
simulations

what do we simulate

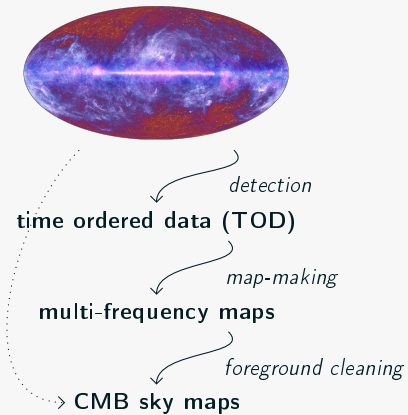


CMB sky maps

what do we simulate

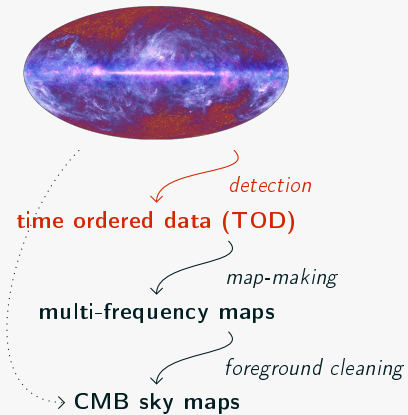


what do we simulate



TOD: collection of the signal detected by *each of the (4508) detectors* during the whole (3-year) mission.

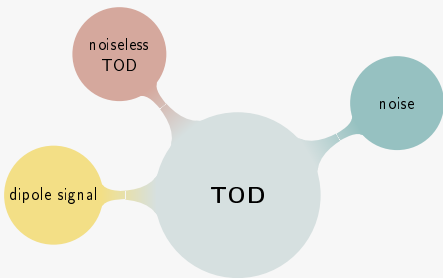
what do we simulate



TOD: collection of the signal detected by *each of the (4508) detectors* during the whole (3-year) mission.

Simulating TOD is crucial in the planning of any CMB experiment: helps studying potential systematic effects.

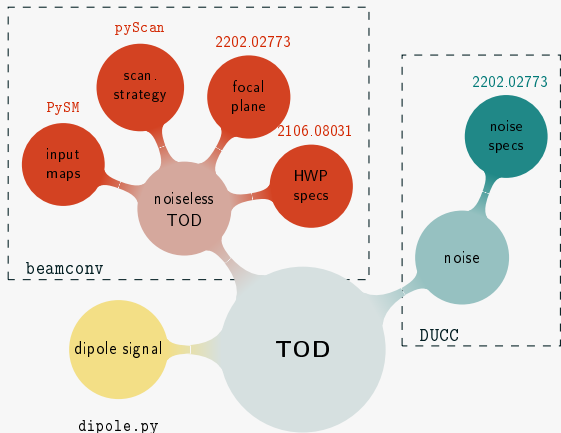
sketch of the pipeline



sketch of the pipeline

beamconv: convolution code simulating TOD for CMB experiments with realistic polarized **beams**, scanning strategies and **HWP**.

DUCC: collection of basic programming tools for numerical computation: fft, sht, healpix, totalconvolve...

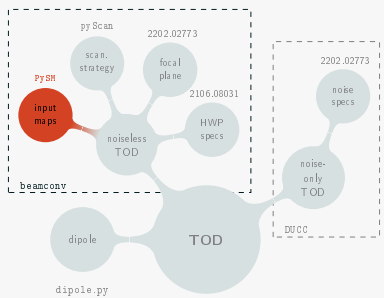


working assumptions

To focus on the impact of **HWP non-idealities**,
we consider a simplified problem:

- ▶ no noise,
- ▶ single frequency,
- ▶ CMB-only,
- ▶ simple beams,
- ▶ HWP aligned to the detector line of sight.

input maps

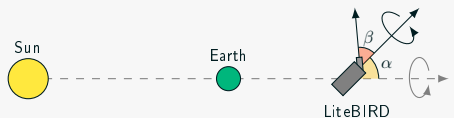
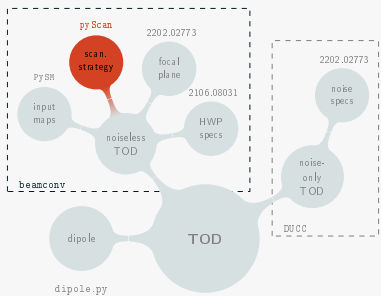


The pipeline can be fed with arbitrary input maps: **CMB**, **foregrounds**, or both.

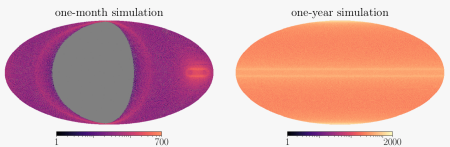
In the paper: I , Q and U input maps with $n_{\text{side}} = 512$ from best-fit 2018 Planck power spectra;

scanning strategy

The pipeline can read or calculate pointings. We implemented some functionalities of pyScan in beamconv to deal with satellite missions.



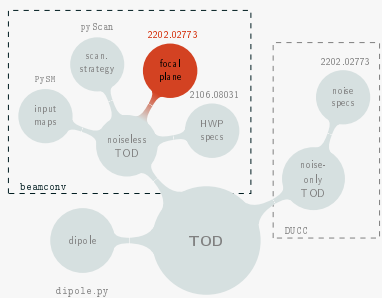
In the paper: 1 year of LiteBIRD-like scanning strategy.



focal plane specifics

The pipeline can read from the Instrument Model Database (IMO):

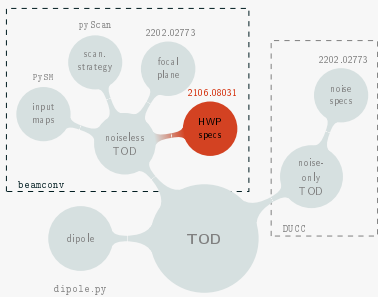
```
{'name': 'M02_030_QA_140T',  
 'wafer': 'M02',  
 'pixel': 30,  
 'pixtype': 'MP1',  
 [...]  
 'pol': 'T',  
 'orient': 'Q',  
 'quat': [1, 0, 0, 0]}
```



In the paper: 160 dets from M1-140.

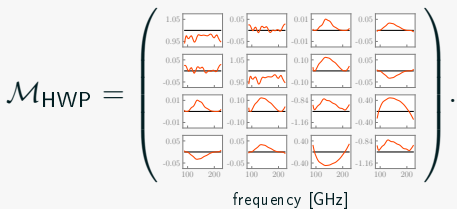
specs.	values
f_{samp}	19 Hz
HWP rpm	39
FWHM	
offset quats.	30.8 arcmin [...]

HWP specifics



In the paper: HWP is assumed to be ideal in the **first** simulation run (ideal TOD) and realistic in the **second** (non-ideal TOD).

Realistic HWP Mueller matrix elements as shown previously:

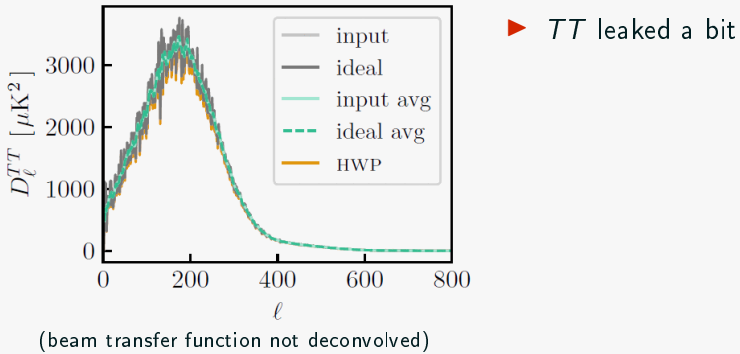


what about maps?

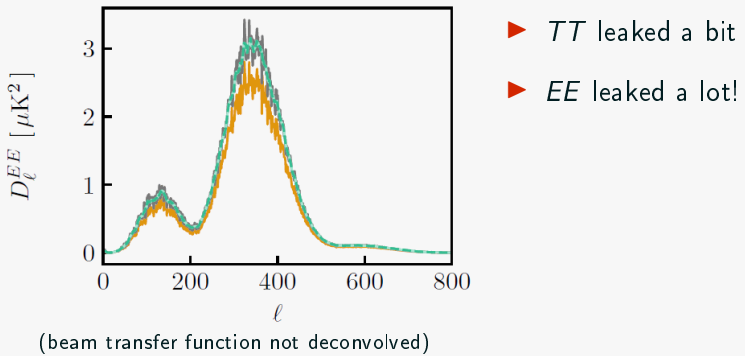
Both ideal and non-ideal TOD processed by **ideal** bin-averaging map-maker.



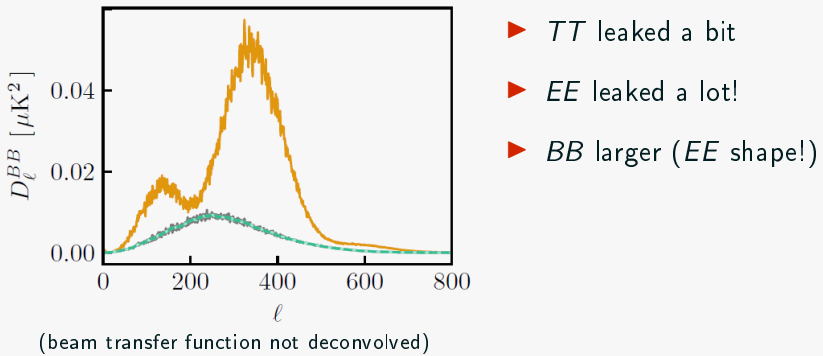
ideal vs non-ideal output spectra (1)



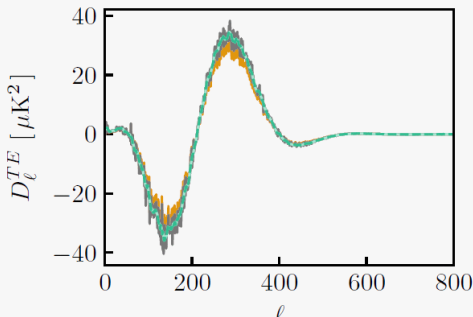
ideal vs non-ideal output spectra (1)



ideal vs non-ideal output spectra (1)



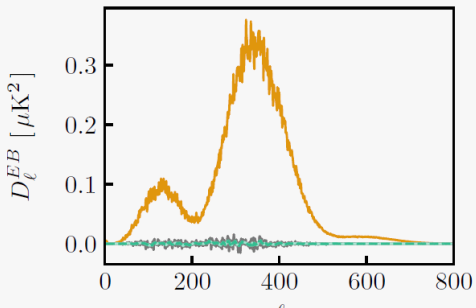
ideal vs non-ideal output spectra (1)



- ▶ *TT* leaked a bit
- ▶ *EE* leaked a lot!
- ▶ *BB* larger (*EE* shape!)
- ▶ *TE* leaked a bit

(beam transfer function not deconvolved)

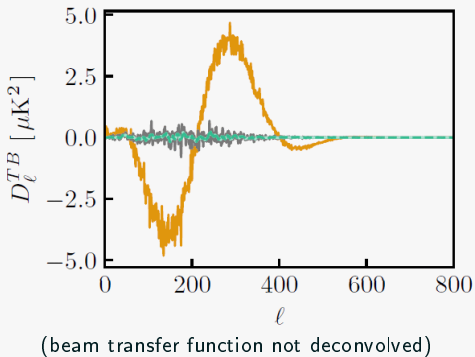
ideal vs non-ideal output spectra (1)



(beam transfer function not deconvolved)

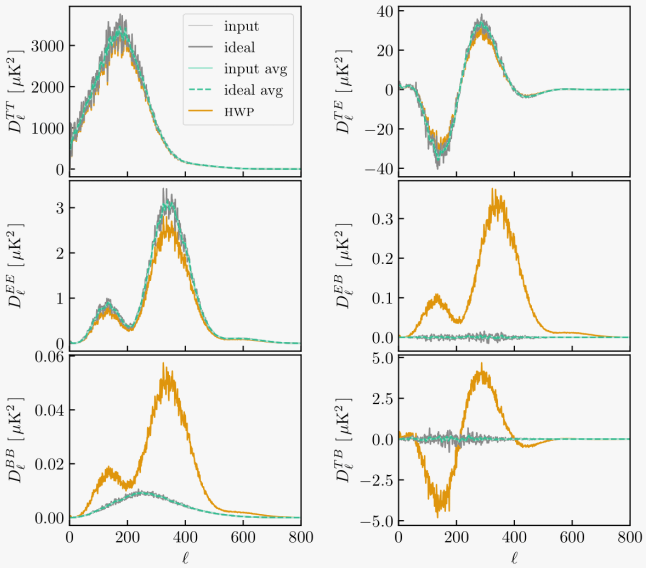
- ▶ TT leaked a bit
- ▶ EE leaked a lot!
- ▶ BB larger (EE shape!)
- ▶ TE leaked a bit
- ▶ EB non-zero!

ideal vs non-ideal output spectra (1)



- ▶ TT leaked a bit
- ▶ EE leaked a lot!
- ▶ BB larger (EE shape!)
- ▶ TE leaked a bit
- ▶ EB non-zero!
- ▶ TB non-zero!

ideal vs non-ideal output spectra (2)



how can we understand this?

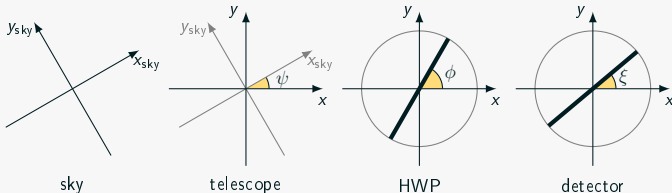
modeling the TOD

How `beamconv` computes the TOD:

$$d_t = \sum_{s\ell m} \left[B_{\ell s}^I a_{\ell m}^I + \frac{1}{2} (-_2 B_{\ell s}^P {}_2 a_{\ell m}^P + {}_2 B_{\ell s}^P {}_{-2} a_{\ell m}^P) + B_{\ell s}^V a_{\ell m}^V \right] \sqrt{\frac{4\pi}{2\ell+1}} e^{-is\psi_t} {}_s Y_{\ell m}(\theta_t, \phi_t),$$

beam coefficients (or combinations of them if HWP non-ideal).

In the paper: $d = (1 \ 0 \ 0) \cdot \mathcal{M}_{\text{det}} \mathcal{R}_{\xi-\phi} \mathcal{M}_{\text{HWP}} \mathcal{R}_{\phi+\psi} \cdot S.$



modeling the observed maps

(minimal) TOD: signal detected by 4 detectors.

map-maker: bin-averaging assuming ideal HWP.

estimated output maps: linear combination of $\{I, Q, U\}_{\text{in}}$.

$$\begin{pmatrix} d^{(0)} \\ d^{(90)} \\ d^{(45)} \\ d^{(135)} \end{pmatrix} = \begin{pmatrix} (1 \ 0 \ 0) \cdot \mathcal{M}_{\text{det}} \mathcal{R}_{0-\phi} \mathcal{M}_{\text{HWP}} \mathcal{R}_{\phi+\psi} \\ (1 \ 0 \ 0) \cdot \mathcal{M}_{\text{det}} \mathcal{R}_{90-\phi} \mathcal{M}_{\text{HWP}} \mathcal{R}_{\phi+\psi} \\ (1 \ 0 \ 0) \cdot \mathcal{M}_{\text{det}} \mathcal{R}_{45-\phi} \mathcal{M}_{\text{HWP}} \mathcal{R}_{\phi+\psi} \\ (1 \ 0 \ 0) \cdot \mathcal{M}_{\text{det}} \mathcal{R}_{135-\phi} \mathcal{M}_{\text{HWP}} \mathcal{R}_{\phi+\psi} \end{pmatrix} \cdot \begin{pmatrix} I_{\text{in}} \\ Q_{\text{in}} \\ U_{\text{in}} \end{pmatrix}$$

Being *ideal*, map-making amounts to apply $(\hat{A}^T \hat{A})^{-1} \hat{A}^T$ to the TOD:

$$\hat{S} = (\hat{A}^T \hat{A})^{-1} \hat{A}^T A \cdot S.$$

estimated output maps

$$\hat{I} = m_{ii} l_{in} + (m_{iq} Q_{in} + m_{iu} U_{in}) \cos(2\alpha) + (m_{iq} U_{in} - m_{iu} Q_{in}) \sin(2\alpha),$$

$$\begin{aligned}\hat{Q} = \frac{1}{2} & \left\{ (m_{qq} - m_{uu}) Q_{in} + (m_{qu} + m_{uq}) U_{in} + 2 m_{qi} l_{in} \cos(2\alpha) + 2 m_{ui} l_{in} \sin(2\alpha) \right. \\ & + [(m_{qq} + m_{uu}) Q_{in} + (m_{qu} - m_{uq}) U_{in}] \cos(4\alpha) \\ & \left. + [-(m_{qu} - m_{uq}) Q_{in} + (m_{qq} + m_{uu}) U_{in}] \sin(4\alpha) \right\},\end{aligned}$$

$$\begin{aligned}\hat{U} = \frac{1}{2} & \left\{ (m_{qq} - m_{uu}) U_{in} - (m_{qu} + m_{uq}) Q_{in} - 2 m_{ui} l_{in} \cos(2\alpha) + 2 m_{qi} l_{in} \sin(2\alpha) \right. \\ & + [-(m_{qq} + m_{uu}) U_{in} + (m_{qu} - m_{uq}) Q_{in}] \cos(4\alpha) \\ & \left. + [(m_{qu} - m_{uq}) U_{in} + (m_{qq} + m_{uu}) Q_{in}] \sin(4\alpha) \right\},\end{aligned}$$

where $\alpha = \phi + \psi$. For **good** coverage and **rapidly spinning** HWP:

$$\hat{S} \simeq \begin{pmatrix} m_{ii} l_{in} \\ [(m_{qq} - m_{uu}) Q_{in} + (m_{qu} + m_{uq}) U_{in}] / 2 \\ [-(m_{qu} + m_{uq}) Q_{in} + (m_{qq} - m_{uu}) U_{in}] / 2 \end{pmatrix}.$$

equations for the \widehat{C}_ℓ s

Expanding \widehat{S} in spherical harmonics:

$$\widehat{C}_\ell^{TT} \simeq m_{ii}^2 C_{\ell,\text{in}}^{TT},$$

$$\widehat{C}_\ell^{EE} \simeq \frac{(m_{qq} - m_{uu})^2}{4} C_{\ell,\text{in}}^{EE} + \frac{(m_{qu} + m_{uq})^2}{4} C_{\ell,\text{in}}^{BB} + \frac{(m_{qq} - m_{uu})(m_{qu} + m_{uq})}{2} C_{\ell,\text{in}}^{EB},$$

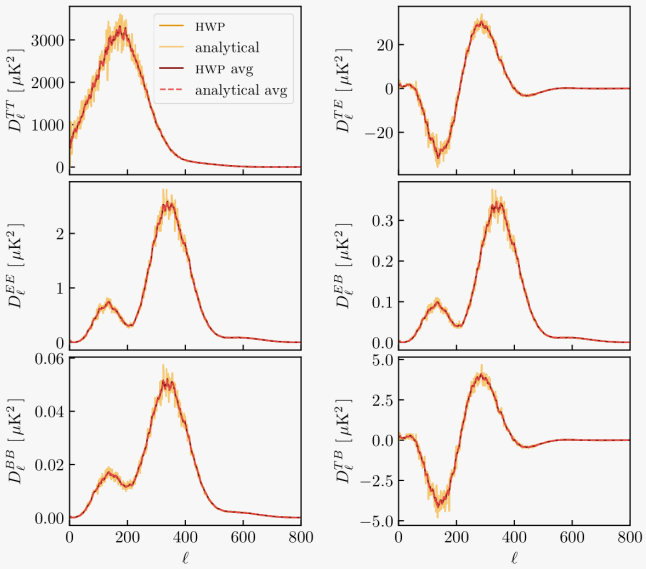
$$\widehat{C}_\ell^{BB} \simeq \frac{(m_{qq} - m_{uu})^2}{4} C_{\ell,\text{in}}^{BB} + \frac{(m_{qu} + m_{uq})^2}{4} C_{\ell,\text{in}}^{EE} - \frac{(m_{qq} - m_{uu})(m_{qu} + m_{uq})}{2} C_{\ell,\text{in}}^{EB},$$

$$\widehat{C}_\ell^{TE} \simeq \frac{m_{ii}(m_{qq} - m_{uu})}{2} C_{\ell,\text{in}}^{TE} + \frac{m_{ii}(m_{qu} + m_{uq})}{2} C_{\ell,\text{in}}^{TB},$$

$$\widehat{C}_\ell^{EB} \simeq \frac{(m_{qq} - m_{uu})^2 - (m_{qu} + m_{uq})^2}{4} C_{\ell,\text{in}}^{EB} - \frac{(m_{qq} - m_{uu})(m_{qu} + m_{uq})}{2} (C_{\ell,\text{in}}^{EE} - C_{\ell,\text{in}}^{BB}),$$

$$\widehat{C}_\ell^{TB} \simeq \frac{m_{ii}(m_{qq} - m_{uu})}{2} C_{\ell,\text{in}}^{TB} - \frac{m_{ii}(m_{qu} + m_{uq})}{2} C_{\ell,\text{in}}^{TE}.$$

analytical vs non-ideal output spectra



impact on cosmic birefringence

HWP-induced miscalibration

Analytic \hat{C}_ℓ s satisfy the relations:

$$\begin{cases} \hat{C}_\ell^{EB} \simeq \tan(4\hat{\theta}) [\hat{C}_\ell^{EE} - \hat{C}_\ell^{BB}] / 2 \\ \hat{C}_\ell^{TB} \simeq \tan(2\hat{\theta}) \hat{C}_\ell^{TE} \end{cases}$$

The HWP induces an additional miscalibration,
degenerate with cosmic birefringence and polarization angle
miscalibration!

HWP-induced miscalibration

Analytic \hat{C}_ℓ s satisfy the relations:

$$\begin{cases} \hat{C}_\ell^{EB} \simeq \tan(4\hat{\theta}) [\hat{C}_\ell^{EE} - \hat{C}_\ell^{BB}] / 2 \\ \hat{C}_\ell^{TB} \simeq \tan(2\hat{\theta}) \hat{C}_\ell^{TE} \end{cases}$$

our formulae suggest
 $\hat{\theta} \equiv -\frac{1}{2} \arctan \frac{m_{qu} + m_{uq}}{m_{qq} - m_{uu}} \sim 3.8^\circ$,
compatibly with simulations.

The HWP induces an additional miscalibration,
degenerate with cosmic birefringence and polarization angle
miscalibration!

This doesn't mean that the HWP will keep us from measuring β ,
but it shows how important it is to carefully calibrate \mathcal{M}_{HWP} .

simple generalizations

including frequency dependence

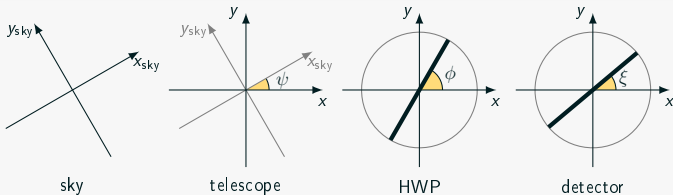
How does $d = (1 \ 0 \ 0) \cdot \mathcal{M}_{\text{det}} \mathcal{R}_{\xi-\phi} \mathcal{M}_{\text{HWP}} \mathcal{R}_{\phi+\psi} \cdot S$ change when the **frequency dependence** of \mathcal{M}_{HWP} and signal is taken into account?

$$d = (1 \ 0 \ 0) \cdot \mathcal{M}_{\text{det}} \mathcal{R}_{\xi-\phi} \int d\nu \mathcal{M}_{\text{HWP}}(\nu) \mathcal{R}_{\phi+\psi} \cdot S(\nu).$$

Assuming an ideal map-maker and retracing the same steps as before:

$$\hat{\theta} = -\frac{1}{2} \arctan \frac{\langle m_{qu} + m_{uq} \rangle}{\langle m_{qq} - m_{uu} \rangle}, \quad \text{where } \langle \cdot \rangle = \int d\nu \cdot (\nu) S(\nu).$$

instrument miscalibration



So far, we assumed $\begin{cases} \hat{\psi} \equiv \psi, \\ \hat{\phi} \equiv \phi, \\ \hat{\xi} \equiv \xi, \end{cases}$ but more generally $\begin{cases} \hat{\psi} \equiv \psi + \delta\phi, \\ \hat{\phi} \equiv \phi + \delta\psi, \\ \hat{\xi} \equiv \xi + \delta\xi. \end{cases}$

Taking such (frequency-independent) deviations into account:

$$\hat{\theta} = -\frac{1}{2} \arctan \frac{\langle m_{qu} + m_{uq} \rangle}{\langle m_{qq} - m_{uu} \rangle} + \delta\theta, \quad \text{where } \delta\theta \equiv \delta\xi - \delta\psi - 2\delta\phi.$$

steps forward

Even *more general* generalizations worth exploring:

- ▶ including a realistic band pass,
- ▶ allowing for miscalibrations to depend on ν .

For how long can we push the analytical formulae?

the importance of calibration

how does the map-model change

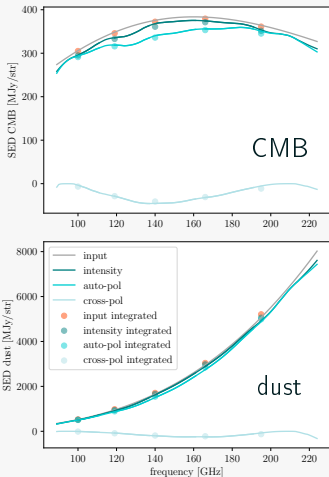
Without HWP: $\begin{pmatrix} I_j \\ Q_j \\ U_j \end{pmatrix} = \sum_{\lambda} g_{\lambda} \begin{pmatrix} I_{\lambda} \\ Q_{\lambda} \\ U_{\lambda} \end{pmatrix} + n,$

With HWP: $\begin{pmatrix} I_j \\ Q_j \\ U_j \end{pmatrix} = \sum_{\lambda} \begin{pmatrix} g_{\lambda}^{ii} & 0 & 0 \\ 0 & g_{\lambda}^{qq-uu} & g_{\lambda}^{qu+uq} \\ 0 & g_{\lambda}^{qu+uq} & g_{\lambda}^{qq-uu} \end{pmatrix} \begin{pmatrix} I_{\lambda} \\ Q_{\lambda} \\ U_{\lambda} \end{pmatrix} + n,$

where $g_{\lambda} = \frac{\int d\nu G(\nu) S_{\lambda}(\nu)}{\int d\nu G(\nu)}$, $g_{\lambda}^{ii} = \frac{\int d\nu G(\nu) m_{ii}(\nu) S_{\lambda}(\nu)}{\int d\nu G(\nu)}$, and so on.

HWP non-idealities contribute to gain, polarization-efficiency and cross-polarization leakage.

effective SEDs



$$\sum_{\lambda} \begin{pmatrix} g_{\lambda}^{ii} & 0 & 0 \\ 0 & g_{\lambda}^{qq-uu} & g_{\lambda}^{qu+uq} \\ 0 & g_{\lambda}^{qu+uq} & g_{\lambda}^{qq-uu} \end{pmatrix} \begin{pmatrix} I_{\lambda} \\ Q_{\lambda} \\ U_{\lambda} \end{pmatrix} + n,$$

- ▶ Since all these effects are frequency dependent, they affect each component differently,
- ▶ An imprecise calibration of \mathcal{M}_{HWP} can lead to complications in the component separation step.

- ▶ we are now provided with a **simulation pipeline** that can be easily adapted to study more complex problems (adding noise, more realistic beams...);
- ▶ the **analytical formulae** represent an alternative tool to study the same problems more effectively (but approximately);
- ▶ obvious application: exploiting the analytical formulae to derive **calibration requirements** for the HWP Mueller matrix elements, so that they don't prevent us from detecting ***B*-modes**, measuring **cosmic birefringence**, nor spoil the **foreground cleaning** procedure.